GENERALIZED SATURATION PROPERTIES OF PURE FLUIDS VIA CUBIC EQUATIONS OF STATE

MARIA A. BARRUFET, PHILIP T. EUBANK
Texas A&M University
College Station, TX 77843

THE MAXWELL CRITERIA require that each cubic equation of state (EOS) has unique, reduced saturation properties when its constants are fixed by the usual critical constraints. For example, a numerical reduced vapor pressure curve results as a function of reduced temperature. Use of independent, empirical EOS and vapor pressure equations has caused thermodynamic inconsistencies in previous correlations.

First, this work shows that some simplifications result when the reduced densities of the saturated liquid and vapor are replaced by their sum

$$s \equiv (\rho_{r,l} + \rho_{r,v})$$

and their difference

$$w \equiv (\rho_{r,l} - \rho_{r,v})$$

Second, we tabulated a complete set of saturation properties calculated from the van der Waals EOS.

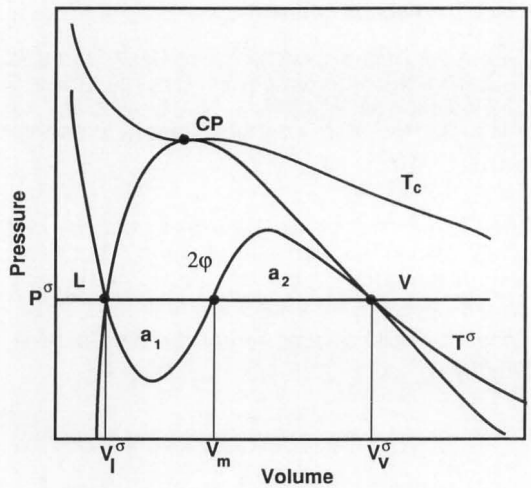

FIGURE 1. A qualitative pressure-volume diagram for a pure substance indicating the coexistence curve with the Maxwell equal area constraint.

Maria A. Barrufet is an engineering research associate at Texas A&M University. She received her BS and MS degrees from the National University of Salta and from the Southern National University of Bahia Blanca (both in Argentina) and her PhD from Texas A&M University. Her research interests are prediction of thermophysical properties of fluid mixtures, heat and reaction engineering, and software development with engineering applications.

Philip T. (Toby) Eubank is professor of chemical engineering at Texas A&M University. He received his BS degree from Rose-Hulman Institute and his PhD from Northwestern University. His research interests are in the thermo-physical properties of fluids and fluid mixtures plus electrical discharge machining.

These properties include reduced vapor pressure

$$P_r^\sigma, \quad \left(dP_r^\sigma / dT_r\right), \quad \rho_{r,l}, \quad \rho_{r,v}$$

reduced heats of vaporization

$$(\lambda / RT_c), \quad \Delta_J C_{v,v}$$

or the jump in the heat capacity from the single to the two-phase side of the vapor pressure curve,

$$\Delta_J C_{v,l}$$

all as functions of T_r (T_r from 0.4 to 0.8 at 0.04 intervals and T_r from 0.8 to unity at 0.02 intervals).

For other cubic EOS such as Redlich-Kwong (RK), Soave-Redlich-Kwong (SRK), and Peng-Robinson (PR), we provided the same set of saturation properties as for the van de Waals case, although for a single reduced temperature of $T_r = 0.8$. For these last three equations we also give the

$$\left(C_{v,\alpha}^{(1)} - C_v^*\right)/R$$

or isochoric heat capacity of the saturated vapor or liquid (α = v or l) from the single-phase side w.r.t. the perfect gas value C_v^* at the same temperature. For SRK and PR equations we used accentric factors

ω = 0.0, 0.2, 0.4, and 0.6.

Finally, graphs of these results are presented for comparison with experimental results for a number of common compounds ranging from argon to water. The successes and failures of the various cubic EOS are shown clearly for a variety of compounds ranging from spherical molecules to highly-polar, hydrogen-bonding species.

INTRODUCTION

Vapor-liquid equilibrium (VLE) calculations of a pure substance through an EOS are usually made by the same trial and error procedures used to calculate VLE for mixtures. The iteration variables are usually pressure (P), (when the temperature (T) is provided), or T when the pressure is known. A pressure (or T) is continuously updated in order to satisfy the equal fugacity criteria at equilibrium. For each attempted P (or T), one must evaluate liquid and vapor densities which in turn are used in the evaluation of fugacities.

Any empirical EOS which is fitting both liquid and vapor densities will exhibit van der Waals loops in the two-phase region. The isothermal form of a polynomial EOS must be of odd order in P(V) in order to satisfy mechanical stability criteria for both phases (*i.e.*, $(\partial P/\partial V)_T < 0$, as can be observed in Figure 1). Figure 1 shows qualitatively the Maxwell equal-area constraint (or equality of the liquid and vapor fugacities) for cubic EOS. The two "humps" in the two-phase region are characteristics of a cubic equation constrained at the critical point; they are called the van der Waals loops in honor of the first cubic EOS. A fifth degree polynomial would present four of these "humps," a seventh degree six, and so forth.

The total derivative of the Gibbs' free energy for a pure substance is

$$dG = -SdT + VdP \tag{1}$$

A phase change, such as vaporization or melting, for a pure substance occurs at constant temperature and pressure. The specific properties of the thermodynamic functions (A, H, S, *etc.*) will be different for the two equilibrium phases except for the Gibbs' free energy, as can be observed by applying the above equation at constant T and P. This is equivalent to the equilibrium criterium of equality of fugacities since

$$dG = RT\,d\,ln\,f \tag{2}$$

The Gibbs free energy can be expressed in terms of the thermodynamic functions as

$$G = A + PV \tag{3}$$

where A is the Helmholtz function and V is the specific or molar volume. Differentiation of this equation at constant pressure and temperature gives

$$[dG = dA + PdV]_{T,P} = 0 \tag{4}$$

Integration between the equilibrium vapor and liquid phases provides

$$\int_{A_v}^{A_l} dA = -\int_{V^\sigma_{r,v}}^{V^\sigma_{r,l}} PdV = P^\sigma\left(V^\sigma_{r,v} - V^\sigma_{r,l}\right) \tag{5}$$

Because the right-hand side of this equation is the area of a rectangle, $a_1 = a_2$ as in Figure 1.

Cubic EOS are the simplest polynomials that can satisfy Maxwell's criteria. The capabilities of the available cubic EOS vary from equation to equation, particularly in the calculation of liquid densities. The purpose of this study is to evaluate some of the most popular EOS of the van der Waals type with regard to their VLE predictions. The studied equations were

TABLE 1: Generalized Cubic Equations of State (EOS)

$$P = \frac{RT}{(V - b_1)} - \frac{a_c\left[\alpha(T_{r,\omega})\right]^2}{(V - b_2)(V - b_3)}$$

EOS	b_1	b_2	b_3	a_c	$\alpha(T_{r,\omega})$	Z_c
VdW	$.12500\,RT_c/P_c$	0	0	$.42188\,R^2T_c^{\,2}/P_c$	1	3/8
RK	$.08664\,RT_c/P_c$	$-b_1$	0	$.42748\,R^2T_c^{\,2}/P_c$	$T_r^{-1/4}$	1/3
SRK	$.08664\,RT_c/P_c$	$-b_1$	0	$.42748\,R^2T_c^{\,2}/P_c$	$1+f_s(\omega)\left(1-\sqrt{T_r}\right)$	1/3
PR	$.07780\,RT_c/P_c$	$-b_1 \pm \sqrt{2}\,b_1$	$-b_1 \pm \sqrt{2}\,b_1$	$.45724\,R^2T_c^{\,2}/P_c$	$1+f_p(\omega)\left(1-\sqrt{T_r}\right)$	.307

$f_s(\omega) = 0.480 + 1.574\,\omega - 0.176\omega^2$

$f_p(\omega) = 0.37464 + 1.54226\,\omega - 0.26992\omega^2$

van der Waals (VdW), Redlich-Kwong (RK), Soave-Redlich-Kwong (SRK) and Peng-Robinson (PR). Because we forced these equations to satisfy the critical constraints they can be written in a generic way using characteristics parameters in terms of the critical constants as indicated in Table 1.

PROCEDURE

In this work, we show an alternative way of solving the classical VLE problem which is much simpler and faster. The saturation properties are presented in a reduced form, which allows the reader to compare their performance with any number of compounds by merely scaling these properties by the critical parameters of the substance in question.

The reduced densities of the vapor and the liquid phases are replaced by two new variables:

the sum

$$s \equiv \rho_{r,l} + \rho_{r,v}$$

and the width

$$w \equiv \rho_{r,l} - \rho_{r,v}$$

of the saturation curve on a temperature/density diagram. A simple relation is obtained between w and s from the EOS applied to the liquid and the vapor phases, after equating the pressures. For instance, after substituting the two new variables in van der Waals' EOS we obtain

$$w^2 = s^2 - 32\,T_r/s + 36 - 12s \qquad (6)$$

When this relation is placed into the equation derived from application of the Maxwell equal-area criteria, it provides a function of a single variable which can be zeroed by any numerical technique (*e.g.*, the Newton-Raphson method or bisection algorithms).

For example, from the VdW EOS this single variable function becomes

$$ln\left[\frac{s(6-s) - (16\,T_r/3) + sw}{s(6-s) - (16\,T_r/3) - sw}\right] - 3\,(6-s)\,w/8\,T_r = 0 \qquad (7)$$

with w from Eq. (6).

An efficient way of calculating VLE using this method is to step down from the critical temperature ($T_r = 1$) for which the value of s is known ($s = 2$), and use this as an initial estimate for the next temperature. A continuation algorithm may be begun in this way by using only a hand calculator. Linearity of s

TABLE 2: Predicted Reduced Saturation Properties From Van Der Waals Equation of State

T_r^σ	P_r^σ	$V_{r,v}^\sigma$	$V_{r,\ell}^\sigma$	$\left(\frac{dP_r}{dT_r}\right)^\sigma$	$\frac{\lambda}{RT_c}$	$\left(\frac{dV_{r,v}}{dT_r}\right)^\sigma$	$\left(\frac{dV_{r,\ell}}{dT_r}\right)^\sigma$	$\frac{\Delta_J C_{v,v}}{R}$	$\frac{\Delta_J C_{v,\ell}}{R}$	$\left(\frac{d^2P_r}{dT_r^2}\right)^\sigma$	$\left(\frac{\partial P_r}{\partial V_{r,v}}\right)^\sigma_{T_r}$	$\left(\frac{\partial P_r}{\partial V_{r,\ell}}\right)^\sigma_{T_r}$
1.00	.10000E+01	.10000E+01	.10000E+01	.40000E+01	.00000E+00	$-\infty$	∞	.45455E+01*	.44554E+00*	.95972E+01*	.00000E+00	.00000E+00
.98	.92191E+00	.13761E+01	.77554E+00	.38091E+01	.84070E+00	−.12412E+02	.44304E+01	.57100E+01	.36166E+01	.94849E+01	−.10086E+00	−.50136E+00
.96	.84762E+00	.16118E+01	.70819E+00	.36206E+01	.11778E+01	−.11510E+02	.26352E+01	.63598E+01	.33139E+01	.93632E+01	−.13335E+00	−.13256E+01
.94	.77707E+00	.18438E+01	.66369E+00	.34347E+01	.14288E+01	−.11799E+02	.18970E+01	.69425E+01	.31010E+01	.92344E+01	−.14148E+00	−.24446E+01
.92	.71021E+00	.20869E+01	.63022E+00	.32513E+01	.16340E+01	−.12570E+02	.14834E+01	.75050E+01	.29327E+01	.90982E+01	−.13768E+00	−.38633E+01
.90	.64700E+00	.23488E+01	.60340E+00	.30708E+01	.18090E+01	−.13676E+02	.12161E+01	.80669E+01	.27922E+01	.89541E+01	−.12779E+00	−.55945E+01
.88	.58736E+00	.26360E+01	.58106E+00	.28932E+01	.19619E+01	−.15088E+02	.10282E+01	.86393E+01	.26708E+01	.88015E+01	−.11500E+00	−.76555E+01
.86	.53125E+00	.29545E+01	.56195E+00	.27188E+01	.20978E+01	−.16822E+02	.88863E+00	.92302E+01	.25636E+01	.86400E+01	−.10115E+00	−.10066E+02
.84	.47859E+00	.33113E+01	.54530E+00	.25477E+01	.22197E+01	−.18919E+02	.78072E+00	.98461E+01	.24673E+01	.84690E+01	−.87331E−01	−.12851E+02
.82	.42932E+00	.37141E+01	.53058E+00	.23801E+01	.23299E+01	−.21444E+02	.69475E+00	.10493E+02	.23798E+01	.82881E+01	−.74207E−01	−.16034E+02
.80	.38336E+00	.41725E+01	.51741E+00	.22162E+01	.24301E+01	−.24486E+02	.62465E+00	.11177E+02	.22994E+01	.80966E+01	−.62143E−01	−.19644E+02
.76	.30108E+00	.53041E+01	.49469E+00	.19005E+01	.26050E+01	−.32622E+02	.51724E+00	.12682E+02	.21560E+01	.76795E+01	−.41814E−01	−.28277E+02
.72	.23108E+00	.68354E+01	.47565E+00	.16025E+01	.27517E+01	−.44780E+02	.43888E+00	.14417E+02	.20305E+01	.72132E+01	−.26628E−01	−.39043E+02
.68	.17262E+00	.89734E+01	.45933E+00	.13242E+01	.28750E+01	−.63524E+02	.37930E+00	.16451E+02	.19189E+01	.66933E+01	−.15987E−01	−.52307E+02
.64	.12485E+00	.12066E+02	.44513E+00	.10678E+01	.29782E+01	−.93577E+02	.33254E+00	.18877E+02	.18184E+01	.61163E+01	−.89822E−02	−.68516E+02
.60	.86869E−01	.16729E+02	.43261E+00	.83568E+00	.30641E+01	−.14410E+03	.29496E+00	.21821E+02	.17272E+01	.54803E+01	−.46707E−02	−.88236E+02
.56	.57645E−01	.24110E+02	.42145E+00	.63015E+00	.31348E+01	−.23403E+03	.26414E+00	.25458E+02	.16438E+01	.47871E+01	−.22134E−02	−.11219E+03
.52	.36073E−01	.36517E+02	.41141E+00	.45339E+00	.31921E+01	−.40569E+03	.23849E+00	.30037E+02	.15673E+01	.40437E+01	−.93591E−03	−.14131E+03
.48	.20967E−01	.58969E+02	.40231E+00	.30713E+00	.32377E+01	−.76275E+03	.21684E+00	.35923E+02	.14969E+01	.32656E+01	−.34303E−03	−.17686E+03
.44	.11084E−01	.10358E+03	.39402E+00	.19225E+00	.32733E+01	−.15901E+04	.19840E+00	.43661E+02	.14322E+01	.24802E+01	−.10466E−03	−.22052E+03
.40	.51745E−02	.20363E+03	.38641E+00	.10825E+00	.33003E+01	−.37906E+04	.18253E+00	.54094E+02	.13727E+01	.17293E+01	−.25098E−04	−.27467E+03

with T_r, the law of rectilinear diameters, is helpful for sequential temperature calculations. However, cubic EOS do not provide exact compliance with rectilinear diameter except in the immediate critical region.

Knowledge of s and w allows back calculation of $\rho_{r,l}$ and $\rho_{r,v}$ and the reduced vapor pressure from the EOS itself. This outlined procedure has been followed for all the EOS listed in Table 1. For the SRK and PR equations we calculated equilibrium properties at acentric factors of $\omega = 0.0$, 0.2, 0.4 and 0.6.

For Redlich-Kwong EOS, the relation between s and w is given by a quartic equation. However, because this equation does not have odd terms in w, it can easily be solved as a quadratic in y with $y = w^2$

$$(a)(y^2) + b(T_r, s)(y) + c(T_r, s) = 0 \qquad (8)$$

where

$$a = \gamma_1 \gamma_2^3$$

$$-b = 4T_r^{1.5}\gamma_2^2 - 2\gamma_1\gamma_2\left(2+\gamma_2^2 s^2\right)$$

$$-c = s\gamma_1\left(2-\gamma_2 s\right)^2\left(4+\gamma_2 s\right) - 4T_r^{1.5}\left(2+\gamma_2 s\right)^2 \qquad (9)$$

with

$$\gamma_1 = 1.282441, \qquad \gamma_2 = 0.259921$$

Once w is calculated from this expression it is placed in the equation derived from application of the Maxwell equal-area constraint and that nonlinear equation is solved for the single variable s which for Redlich-Kwong is

$$T_r\left(ln\left[\frac{2(s-w)-\gamma_2(s^2-w^2)}{2(s+w)-\gamma_2(s^2-w^2)}\right] - \frac{4w\gamma_2}{\left(2-\gamma_2 s\right)^2-\left(\gamma_2 w\right)^2}\right) +$$

$$\frac{\gamma_1}{T_r^{0.5}}\left(\frac{ln\left[\dfrac{2+\gamma_2(s+w)}{2+\gamma_2(s-w}\right]}{\gamma_2} + \frac{4w}{\left(2+\gamma_2 s\right)^2-\left(\gamma_2 w\right)^2}\right) = 0 \qquad (10)$$

Table 2 contains a complete set of saturation properties calculated from the Van der Waals EOS. Table 3 contains an example of the saturation properties obtained using the RK, SRK and PR EOS for one re-

TABLE 3

Predicted Reduced Saturation Properties From Classical Cubic EOS at Reduced Temperature $T_r = 0.8$

REDUCED PROPERTY	REDLICH KWONG	SOAVE–REDLICH- KWONG				PENG–ROBINSON			
		$\omega = 0.0$	$\omega = 0.2$	$\omega = 0.4$	$\omega = 0.6$	$\omega = 0.0$	$\omega = 0.2$	$\omega = 0.4$	$\omega = 0.6$
P_r^σ	.24594E+00	.25893E+00	.20117E+00	.15707E+00	.12333E+00	.25789E+00	.19878E+00	.15521E+00	.12289E+00
$V_{r,v}^\sigma$	.79603E+01	.74502E+01	.10029E+02	.13288E+02	.17371E+02	.80567E+01	.10981E+02	.14578E+02	.18910E+02
$V_{r,\ell}^\sigma$	.41194E+00	.41443E+00	.39516E+00	.38057E+00	.36914E+00	.39904E+00	.37983E+00	.36587E+00	.35533E+00
$\left(\frac{dP_r}{dT_r}\right)^\sigma$	.21862E+01	.21592E+01	.20216E+01	.18490E+01	.16646E+01	.21355E+01	.19912E+01	.18180E+01	.16411E+01
$\frac{\lambda}{RT_c}$	.44006E+01	.40698E+01	.52176E+01	.63934E+01	.75818E+01	.40162E+01	.51844E+01	.63456E+01	.74784E+01
$-\left(\frac{dV_{r,v}}{dT_r}\right)^\sigma$	.72483E+02	.63550E+02	.10192E+03	.15671E+03	.23318E+03	.68997E+02	.11209E+03	.17203E+03	.25225E+03
$\left(\frac{dV_{r,\ell}}{dT_r}\right)^\sigma$	.63407E+00	.62219E+00	.58449E+00	.55127E+00	.52218E+00	.60137E+00	.55864E+00	.52310E+00	.49355E+00
$-\left(\frac{C_{v,v}^{(1)}-C_v^\star}{R}\right)$	-.16617E+00	.24828E-01	.28603E-01	.27945E-01	.25326E-01	.21050E-01	.26367E-01	.26618E-01	.24722E-01
$-\left(\frac{C_{v,\ell}^{(1)}-C_v^\star}{R}\right)$	-.25298E+00	.35279E+00	.56557E+00	.75167E+00	.90986E+00	.30114E+00	.53008E+00	.72745E+00	.89315E+00
$\frac{\Delta_J C_{v,v}}{R}$	.33933E+02	.29054E+02	.45892E+02	.66805E+02	.91731E+02	.28595E+02	.45605E+02	.66117E+02	.89610E+02
$\frac{\Delta_J C_{v,\ell}}{R}$	.46097E+01	.41213E+01	.53144E+01	.64638E+01	.75550E+01	.40378E+01	.52281E+01	.63382E+01	.73565E+01
$\left(\frac{d^2P_r}{dT_r^2}\right)^\sigma$	.13393E+02	.13402E+02	.15930E+02	.17660E+02	.18676E+02	.13206E+02	.15701E+02	.17327E+02	.18240E+02
$-\left(\frac{\partial P_r}{\partial V_{r,v}}\right)_{T_r}^\sigma$	.24220E-01	.26854E-01	.16490E-01	.10154E-01	.62976E-02	.24456E-01	.14779E-01	.90961E-02	.57342E-02
$-\left(\frac{\partial P_r}{\partial V_{r,\ell}}\right)_{T_r}^\sigma$	.42996E+02	.39739E+02	.58069E+02	.79396E+02	.10343E+03	.45461E+02	.68210E+02	.94312E+02	.12297E+03

duced temperature (T_r = 0.8). For PR and SRK, we used acentric factors of (ω) 0.0, 0.2, 0.4, and 0.6. The interested reader, however, may obtain from us an unabridged version of Table 3 with a finer grid of ω and a complete range of T_r.

We compared the saturation properties for a number of substances ranging from spherical to highly-polar, hydrogen-bonding species. The critical properties were taken from Ambrose [1, 2]. The sources for the experimental data of water were taken from Haar, *et al.* [3]. Argon, CO_2 and methane were taken from the IUPAC international tables [4], [5], and [6], respectively. For pentane and neopentane, we took the correlated values of [7] and [8], respectively.

Figure 2 is a plot of reduced temperature against reduced density obtained from the VdW, RK, SRK and PR EOS—the last two equations of state with zero acentric factors; this diagram emphasizes the liquid-phase predictions, which are generally poor, particularly for CO_2 and water. Use of the acentric factor in the VLE calculations of SRK and PR EOS slightly improves the liquid-phase predictions. We encourage the reader to compare the performance of all the equations at T_r = 0.8 and at different values of the acentric factor ω where applicable.

The difficulties with all the EOS for the vapor side predictions are enhanced in Figure 3, which shows T_r against Z_r (the reduced compressibility factor). This plot emphasizes the difficulties that cubic EOS, constrained at the CP, have in the prediction of saturation properties. The non-universality of the critical compressibility factor (Z_c) is clearly seen by comparing the spread of the data points as the perfect gas value is approached ($T_r < 0.6$). All the EOS tested produce a unique limiting value which is the inverse of their predicted Z_c.

Once the basic properties

$$\rho_{r,l}, \quad \rho_{r,v}, \quad P_r^{\sigma}$$

are obtained from the Maxwell minimization technique, the rest of reduced saturation properties are obtained sequentially upon application of the Clapeyron equation and standard thermodynamic relations as follows.

ADDITIONAL SATURATION PROPERTIES

The dimensionless heat of vaporization, λ/RT_c, can be calculated using density residual properties:

$$\frac{\lambda}{RT_c} = \frac{H_i^v - H_i^l}{RT_c} = \frac{\left(H_i^r\right)_v - \left(H_i^r\right)_l}{RT_c} \tag{11}$$

Where H_i^r is the residual enthalpy defined as the actual enthalpy minus that of the ideal gas [9]:

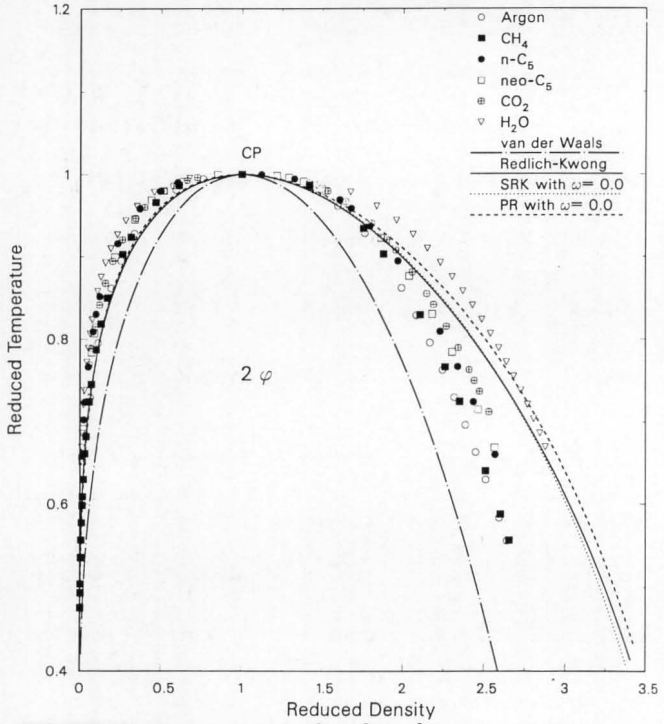

FIGURE 2. Comparison of reduced temperature vs. reduced densities in the coexistence curve.

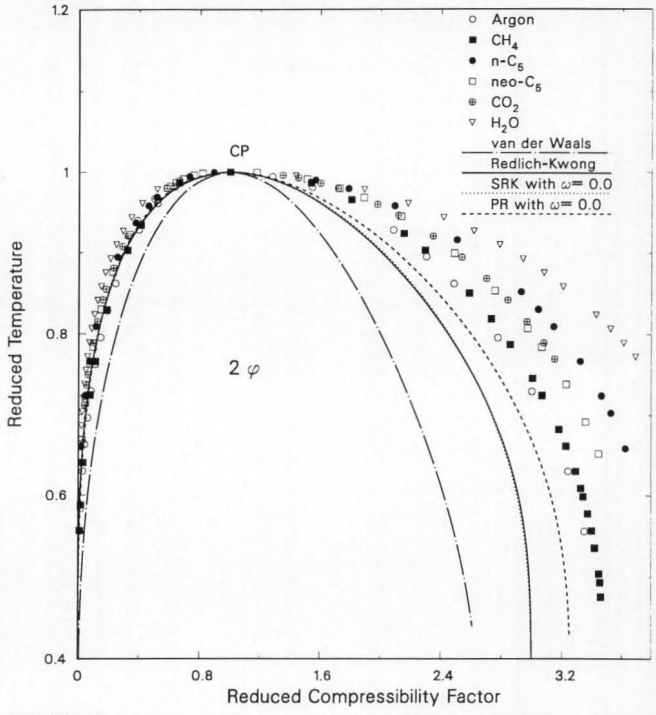

FIGURE 3. Comparison of reduced temperature vs. reduced compressibility factors in the coexistence curve.

$$\left(H_i^r\right)_v = H_i^v - H_i^* \tag{12}$$

The residual enthalpies are evaluated from

$$\frac{\lambda}{RT_c} = T_r \int_{\rho_{r,l}}^{\rho_{r,v}} \left[\left(\frac{\partial Z_r}{\partial T_r}\right)_{\rho_r} \frac{d\rho_r}{\rho_r}\right] + \left(Z_{r,v} - Z_{r,l}\right) \tag{13}$$

This integral is easily evaluated from any of the EOS listed in Table 1 with the limits from the VLE calculations. Upon use of the Clapeyron equation, the dimensionless vapor pressure slope then becomes

$$\left(\frac{dP_r}{dT_r}\right)^\sigma = \left(\frac{\lambda}{RT_c}\right)\left(\frac{1}{Z_c T_r\left(V_{r,v}^\sigma - V_{r,l}^\sigma\right)}\right) \tag{14}$$

The slopes of the saturated liquid and vapor volumes are calculated as

$$\left(\frac{dV_{r,\alpha}}{dT_r}\right)^\sigma = \left[\left(\frac{dP_r}{dT_r}\right)^\sigma - \left(\frac{\partial P_r}{\partial T_r}\right)_{V_r}^\sigma\right]\left[\left(\frac{\partial P_r}{\partial V_{r,\alpha}}\right)_{T_r}^\sigma\right]^{-1} \tag{15}$$

The dimensionless isochoric heat capacity of the vapor evaluated from the single phase side is calculated from

$$\left(\frac{C_{v,v}^{(1)} - C_v^*}{R}\right) = -\int_0^{\rho_{r,\alpha}} \left[\left(\frac{T_r}{\rho_r^2}\right)\left(\frac{\partial^2 P_r}{\partial T_r^2}\right)_{\rho_r}\right] d\rho_r \tag{16}$$

Since the equation of Van der Waals provides straight isochores

$$\left(\frac{\partial^2 P_r}{\partial T_r^2}\right)_{\rho_r} = 0$$

the isochoric heat capacity coincides with the ideal gas heat capacity C_v^*. The jumps in the heat capacities are evaluated as

$$\frac{\Delta_J C_{v,\alpha}}{R} = Z_c T_c \left(\frac{dV_{r,\alpha}}{dT_r}\right)^\sigma \left[\left(\frac{\partial P_r}{\partial T_r}\right)_{V_r}^\sigma - \left(\frac{dP_r}{dT_r}\right)^\sigma\right] \tag{17}$$

In Eq. (12), α indicates that the quantity can be evaluated either for the liquid or for the vapor side.

The isochoric heat capacity for the vapor phase evaluated from the two phase side is not reported in Table 2, but can be calculated as follows:

$$\left(\frac{C_{v,v}^{(2)} - C_v^*}{R}\right) = \frac{\Delta_J C_{v,v}}{R} + \left(\frac{C_{v,v}^{(1)} - C_v^*}{R}\right) \tag{18}$$

with an equivalent expression for the isochoric liquid heat capacity.

A CLASSROOM APPLICATION

This example could be used as a part of a test or a graduate qualification exam. Assuming that the properties of iso-octane can be represented by the Redlich-Kwong EOS, the student is asked to use the generalized saturation properties given in Table 3 to estimate the following quantities at $T_r = 0.8$.

[1] The vapor pressure (in bars), as well as the saturation volumes for the liquid and the vapor phase in (cm^3/mol).

[2] How could he/she verify the consistency of the heat of vaporization λ, given in the table with the corresponding values of the vapor pressure and the saturation volumes?

[3] Using the Redlich-Kwong, derive an expression for the residual isochoric heat capacity ($C_v - C_v^*$), as a function of pressure (or volume) along an isotherm in the gas phase, and calculate the value of C_v for saturated iso-octane vapor at $T_r = 0.8$ as taken from the two-phase side using their derived equation. (Note $C_v^* = 21$ J/mol-K).

DISCUSSION

The limiting values of the saturation properties at the critical point were evaluated analytically or numerically (the starred values). The slope of the vapor pressure curve evaluated at the critical point is collinear to the isochoric slope

$$\left(\frac{\partial P_r}{\partial T_r}\right)_{V_r}^\sigma \Bigg|_{CP}$$

taken from the single phase side. Even though the analytical expression resulting from Clapeyron equation (Eq. (11)) diverges at the CP, this divergence is removed upon application of L'Hopital's rule taking the limit when the reduced densities approach to unity.

The "critical" values for

$$\frac{\Delta_J C_{v,\alpha}}{R} \quad \text{and for} \quad \left(\frac{d^2 P_r}{dT_r^2}\right)^\sigma$$

were evaluated at a reduced temperature of $T_r = 0.9999$ which for most practical applications is sufficiently close to the critical point.

It is well known that the curvature of the isochores

$$\left(\frac{\partial^2 P_r}{\partial T_r^2}\right)_{\rho_r}$$

is negative for gas densities, increases with density becoming zero near the critical density, and then posi-

tive for liquid densities. None of the cubic EOS tested is able to reproduce this feature which is reflected in

$$\left(\frac{C_{v,v}^{(1)} - C_v^*}{R}\right)$$

(since C_v^* is smaller than $\left(C_v^{1,2}\right)_{l,v}$

VdW provides straight isochores everywhere. For the other EOS analyzed, the sign of the curvature is either fixed and negative as in the RK EOS, or temperature dependent as in the PR and SRK EOS. In either case, for a given temperature the sign remains regardless of the density (vapor or liquid). For example, RK provides the right physics for the curvature of vapor densities but fails for the liquid.

The Soave-Redlich-Kwong and Peng-Robinson EOS were designed to give a better representation of the liquid phase behavior. This they do so even with the isochoric curvature

$$\left(\frac{\partial^2 P_r}{\partial T_r^2}\right)_{\rho_r}$$

although not in the full temperature range and at the expense of misrepresenting the vapor curvature. Along any isochore the curvature will be negative for all temperatures above the "switching" temperature, zero itself at this temperature, and positive below. This switching temperature depends upon the acentric factor. Table 4 contains these temperatures for SRK and PR EOS as a function of ω.

CONCLUSIONS

We believe that Table 2 constitutes a most complete "thermodynamic dictionary of reduced saturated properties." Further, we can provide the reader with the unabridged version of Table 3 which shows the real goodness (or weakness) of the most popular equations of state. Our procedures are different and somewhat more general than those of Adachi [10], and Soave [11, 12].

These reduced properties may have multiple uses either as reference values for experimental designs or as valuable information (initial guesses, initiation algorithms) in multicomponent VLE calculations. We have also given the basis for calculating VLE in terms of convenient variables (s and w) that allow the calculations in a much faster and convenient way.

TABLE 4
Reduced Switching Temperature in SRK and PR EOS as a Function of ω

	Soave-Redlich-Kwong		Peng-Robinson	
ω	$f_s(\omega)$	T_r^s	$f_p(\omega)$	T_r^s
0.0	0.48000	0.56035	0.37464	0.54858
0.2	0.78776	0.59106	0.67229	0.58012
0.4	1.08144	0.61625	0.94836	0.60527
0.6	1.36104	0.63727	1.20285	0.62569

$f_s(\omega) = 0.480 + 1.574(\omega - 0.176)(\omega^2)$

$f_p(\omega) = 0.37464 + 1.54226(\omega - 0.26992)(\omega^2)$

ACKNOWLEDGMENTS

Financial support by the National Science Foundation Grant No CBT – 8718204 is gratefully acknowledged. We also thank C. D. Holland, J. C. Holste, and K. R. Hall for their helpful advice.

NOMENCLATURE

A	= Helmholtz free energy function.
$C_{v,v}$	= Isochoric heat capacity of the vapor
$C_{v,l}$	= Isochoric heat capacity of the liquid
EOS	= Equation of State
H_i	= Molar Enthalpy of component i
P,V,T	= Pressure, Volume, Temperature
R	= Universal Gas Constant
VLE	= Vapor Liquid Equilibria
Z	= Compressibility factor

Greek Letters

$\Delta_J C_{v,\alpha}/R$ =	jump in C_v single minus two-phase side
λ/RT_c	= reduced heat of vaporization
ω	= acentric factor
ρ	= density
σ	= property at saturation

Subscripts

c	= critical property
i	= component i
l	= liquid value
r	= reduced property with respect to critical parameters
v	= vapor value

Superscripts

σ	= property at saturation
*	= ideal gas value, or extrapolated value in Table 2.
(1,2)	= single—two phase value
l	= liquid
v	= vapor

REFERENCES

1. Ambrose, D., and R. Townsend, "Critical Temperatures and Pressures of Some Alkanes," *Trans. Faraday Soc.*, **64**, 550 (1968)

2. Ambrose, D., "Vapour Liquid Critical Properties," *Na. Phys. Lab. Report,* No. 107, London (1980)
3. Haar, L., J. S. Gallagher, and G. S. Kell, *NBS/NRC Steam Tables,* McGraw-Hill, New York (1984)
4. Angus, S., B. Armstrong, *IUPAC. International Thermodynamic Tables of the Fluid State: Argon,* **1**, Butterworths, London (1972)
5. Angus, S., B. Armstrong, and K. M. de Reuck, *IUPAC. International Thermodynamic Tables of the Fluid State: Methane,* **5**, Pergamon Press, Oxford (1978)
6. Angus, S., B. Armstrong, and K. M. de Reuck, *IUPAC. International Thermodynamic Tables of the Fluid State: Methane,* **5**, Pergamon Press, Oxford (1978)
7. Das, T. R., C. O. Reed, Jr., and P. T. Eubank, "PVT Surface and Thermodynamic Properties of Neopentane," *J. Chem. Eng. Data,* **22**, 1 (1977a)
8. Das, T. R., C. O. Reed, Jr., and P. T. Eubank, "PVT Surface and Thermodynamic Properties of n-Pentane," *J. Chem. Eng. Data,* **22**, 3 (1977b)
9. Adachi, Y., "Generalization of Soave's Direct Method to Calculate Pure-Compound Vapor Pressures Through Cubic Equations of State," *Fluid Phase Equilibria,* **35** (1987)
10. Soave, G., "Improvement of the van der Waals Equation of State," *Chem. Eng. Sci.,* **39**, 357 (1984)
11. Soave, G., "Direct Calculation of Pure-Compound Vapour Pressures Through Cubic Equations of State," *Fluid Phase Equilibria,* **31**, 203 (1986) ❐

ChE book reviews

TRANSPORT PHENOMENA IN TURBULENT FLOWS: Theory, Experiment, and Numerical Simulation

M. Hirata, N. Kasagi, Editors
Hemisphere Publishing Corp., New York; 921 pages, $150 (1988)

Reviewed by
Robert S. Brodkey
Ohio State University

About one hundred fifty authors have contributed fifty-six general papers and eight keynote addresses to the 2nd International Symposium on Transport Phenomena in Turbulent Flows, held at the University of Tokyo in October, 1987. Over one hundred ten extended abstracts were submitted; thus the volume represents a selection of half of those submitted. The volume (921 pages) was delivered to me for review in less than a year from the date of the symposium; a positive note for the editors, Hirata and Kasagi, and for the publisher, Hemisphere. The copy-ready text varies from papers that are as good as a press-printed journal article to those of poor quality that require the reader to guess at what was intended. One would hope that in the future these few authors could obtain new equipment like a laser printer, or at least a new ribbon. There are quite a few minor typographical errors that might have been eliminated by better proofreading by the authors. Neither the editors nor the publisher are responsible for this.

It was not clear if any of the discussion (not included) at the meeting was incorporated into the papers as they appeared. There is a brief note included that was an outgrowth of a discussion that arose at the meeting.

The editors grouped the contributions into nine sections: fundamentals (5 papers), coherent structures (10), wall shear flow (7), free shear flow (7), scalar and buoyant transport (5), modeling and prediction of turbulent transport (9), numerical simulations of turbulence (4), measurement techniques (6), and turbulent transport in applications (4).

The eight keynote papers are all noteworthy and are: 1) Coherent Structures Associated with Turbulent Transport, by Blackwelder, 2) The Organized Motion and Its Contribution to Transport in Shear Flows, by Antonia, 3) Turbulence Management in Free Shear Flows by Control of Coherent Structures, by Husian, Bridges, and Hussain, 4) Turbulent Transfer to a Wall at Larger Schmidt Numbers, by Hanratty and Vassiliadou, 5) Natural Convection Mass Transfer in an Inclined Enclosure at High Rayleigh Number, by Goldstein, Chiang, and Sayer, 6) Recent Results in the Prediction of Turbulent Separated Flows, by Pletcher, 7) Advances in Turbulent Transport Modeling Based on Direct Simulations of Turbulence, by Reynolds, Rogers, and Sandham, and 8) Investigation of Heat and Momentum Transport in Turbulent Flows Via Numerical Simulations, by Kim.

The topics cover the broad areas of turbulent transport research and thus will find limited use by any one individual. Certainly, institutions that have research interests and programs in the areas will want the volume for library use. About 20% of the contributions are on a variety of fundamentals and the remainder on a wide range of applied problems that involve coupled phenomena and/or a complex geometry. There is a clear increase in the use of computers in experimental and numerical investigations of turbulent flows. The use of large data bases generated on supercomputers is evident.

In the time and space available for this review it was impossible to read all the contributions in detail. Thus, I have concentrated on the keynote lectures and those contributions in the fields that I have worked in. The more senior and well-known authors did speculate on ideas that are neither proven nor necessarily shared by others. They did this honestly, and their efforts are appreciated by this reviewer. Many of the contributions are complete to a degree that they could be considered for publication in the best peer-reviewed journals. There are also papers that are incomplete in their background review and in their understanding of principles. These would not receive consideration for journal publication in their present state.

Continued on page 181.